Migratory Aptitude of the Zr−C Functionalities Bonded to a Macrocyclic Structure: Thermally- and Solvent-Assisted Intra- and Intermolecular Migrations in Dialkyl(dibenzotetramethyltetraazaannulene)zirconium(IV)

Luca Giannini,[†] Euro Solari,[†] Stefania De Angelis,[†] Thomas R. Ward,[§] Carlo Floriani,*[,†] Angiola Chiesi-Villa,[‡] and Corrado Rizzoli[‡]

Contribution from the Institut de Chimie Minérale et Analytique, BCH, Université de Lausanne, CH-1015 Lausanne, Switzerland, and Dipartimento di Chimica, Università di Parma, I-43100 Parma, Italy

Received December 29, 1994[⊗]

Abstract: The Zr−C bond chemistry and, particularly, its migration properties have been investigated where the metal is bonded to the dibenzotetramethyltetraaza[14]annulene (tmtaa) dianion in the model complexes *cis*-[Zr(tmtaa)R_2]. In this respect the [Zr(tmtaa)] fragment has been analyzed in comparison with the well-known [cp_2Zr] moiety, with the support of an extended Hückel analysis. The synthesis of [Zr(tmtaa)R_2] (R = Me, **2**; R = CH_2Ph, **3**) from [Zr(tmtaa)Cl_2] (**1**) has been achieved under highly controlled reaction conditions. Complexes **2** and **3** are thermally labile, and one of the alkyl groups undergoes a thermally-induced migration to one of the imino groups, leading to a trianionic ligand [Zr(R-tmtaa)R] (R = Me, **4**; R = CH_2Ph, **5**). The nature of such complexes has been elucidated by an X-ray analysis on the THF-solvated form of **4**, [Zr(Me-tmtaa)(Me)(THF)] (**6**). Nucleophiles are even more effective in inducing the alkyl migration to the ligand. In the presence of THF or pyridine **5** may be easily converted to [Zr(R_2-tmtaa)] (R = CH_2Ph, **7**), in which both alkyl groups have migrated to the imino groups of the ligand. The use of an excess of LiMe during the alkylation of **1** led to the formation of [Zr(Me_2-tmtaa)···Li-$(THF)_2$] (**8**) *via* the intermediacy of **4**. Complex **8** is a bifunctional carrier of LiMe. The general consequences of two electrophilic sites on the ligand, eventually, in competition with the electrophilic metal have been analyzed. The net charge and electrophilic index are significantly higher for the metal in $[cp_2Zr]^{2+}$ than in $[Zr(tmtaa)]^{2+}$. The relatively higher thermal inertness of **3** allowed us to study the migration of the alkyl group toward the unsaturated incoming nucleophiles, Bu^tNC and CO. The reaction of **3** with Bu^tNC led to the formation of the bis(η^2-iminoacyl) compound [Zr(tmtaa)(η^2-C(Me)=NBu^t)$_2$]. The four low-lying *d* orbitals can accommodate the two η^2-iminoacyl groups. The reaction of **3** with CO gave [Zr(tmtaa)(η^2-OC(CH_2Ph)$_2$)] (**11**) *via* the intermediacy of a very reactive oxycarbene η^2-acyl compound and ultimately gave **12** and **13**, illustrating the reactivity of both zirconium and the iminato carbons in the [Zr(tmtaa)] fragment. The crystallographic details are as follows: **3** is orthorhombic, space group *Pnma*, a = 16.028(3) Å, b = 20.666(4) Å, c = 9.018(2) Å, $\alpha = \beta = \gamma = 90°$, Z = 4, and R = 0.063. **6** is monoclinic, space group $P2_1/n$, a = 19.859(5) Å, b = 14.771(5) Å, c = 9.072(4) Å, $\alpha = \gamma = 90°$, β = 93.85(3)°, Z = 4, and R = 0.044. **7** is monoclinic, space group $C2/c$, a = 23.608(6) Å, b = 9.529(3) Å, c = 19.050(4) Å, $\alpha = \gamma = 90°$, β = 99.30(2)°, Z = 4, and R = 0.046. **10** is triclinic, space group $P\bar{1}$, a = 12.800(4) Å, b = 15.795(5) Å, c = 11.758(1) Å, α = 91.8(2)°, β = 93.56(1)°, γ = 97.81(2)°, Z = 2, and R = 0.042.

Introduction

Group 4 metal organometallic chemistry has made some of the major impacts in providing useful tools for metal-assisted organic transformations.[1] They include stoichiometric reactions, such as hydrozirconation,[2] and catalytic processes, for example titanium- and zirconium-assisted olefin polymerization.[3] The key functionality central to all of these processes is the M−C bond. Looking back through the history of this functionality, one finds essentially two sources, the 'unstabilized' one derived from the alkylation of the metal halides[3] or the protected one attached to the [cp_2M] fragment (cp = η^5-C_5H_5).[1] In the last two decades the [cp_2M] moiety became the representative example of an organometallic fragment usable in all varieties of metal-assisted reactions. In the meantime very few attempts have been made to move out of this convenient fragment and

* To whom correspondence should be addressed.
[†] University of Lausanne.
[§] Present address: Institut für Anorganische Chemie, Universität Bern, CH-3012 Bern, Switzerland.
[‡] University of Parma.
[⊗] Abstract published in *Advance ACS Abstracts*, May 1, 1995.

(1) (a) Reetz, M. T. *Organotitanium Reagents in Organic Synthesis*; Springer: Berlin, Germany, 1986. (b) Wailes, P. C.; Courts, R. P.; Weigold, H. *Organometallic Chemistry of Titanium, Zirconium and Hafnium*; Academic: New York, 1974. (c) Cardin, D. J.; Lappert, M. F.; Raston, C. L. *Chemistry of Organozirconium and Hafnium Compounds*; Wiley: New York, 1986. (d) Buchwald, S. L.; Nielsen, R. B. *Chem. Rev.* **1988**, *88*, 1047. (e) Reetz, M. T. In *Organometallics in Synthesis*; Schlosser, M., Ed.; Wiley: New York, 1994; Chapter 3. (f) Duthaler, R. O.; Hafner, A.; Riediker, M. In *Organic Synthesis via Organometallics*; Dötz, K. H., Hoffmann, R. W., Eds.; Vieweg: Braunschweig, 1991; p 285. (g) Negishi, E.-I. In *Comprehensive Organic Synthesis*; Paquette, L. A., Ed.; Pergamon: Oxford, 1991; Vol. 5, p 1163. (h) Grossman, R. B.; Buchwald, S. L. *J. Org. Chem.* **1992**, *57*, 5803 and references therein. (i) Negishi, E.-I.; Takahashi, T. *Acc. Chem. Res.* **1994**, *27*, 124 and references therein. (j) Schore, N. E. In *Comprehensive Organic Synthesis*; Paquette, L. A., Ed.; Pergamon: Oxford, 1991; Vol. 5, p 1037. (k) Erker, G.; Krüger, C.; Müller, G. *Adv. Organomet. Chem.* **1985**, *24*, 1 and references therein. (l) Swanson, D. R.; Negishi, E. *Organometallics* **1991**, *10*, 825. (m) Erker, G.; Pfaff, R.; Krüger, C.; Werner, S. *Organometallics* **1993**, *12*, 3559. (n) Erker, G.; Noe, R.; Krüger, C.; Werner, S. *Organometallics* **1992**, *11*, 4174. (o) Erker, G.; Pfaff, R. *Organometallics* **1993**, *12*, 1921.

0002-7863/95/1517-5801$09.00/0

to improve upon it. One strategy is the use of alkoxo groups as ancillary ligands;[4] another one makes use of macrocyclic ligands, which until recently have been confined to coordination chemistry in its strictest sense. These macrocycles really only found popular use in the organometallic derivatization of Fe, Ru and Co, Rh couples in porphyrin chemistry,[5] with the other cases being spread over a range of metals. In the case of the group 4 metals, we should mention four major approaches according to chronological order: the use of (i) tetradentate Schiff bases, *i.e.* salen,[6] (ii) dibenzotetramethyltetraaza[14]-annulenes (tmtaa's),[7] (iii) the porphyrin skeleton,[8] (iv) *meso*-octaalkylporphyrinogen.[9]

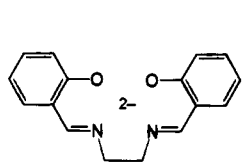

salen

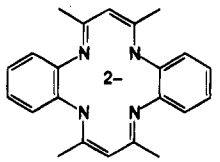

tmtaa

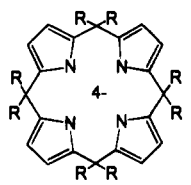

porphyrinogen

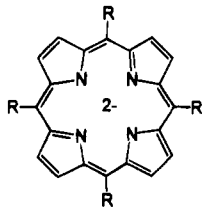

porphyrin

Whilst using tetradentate Schiff bases as ancillary ligands in the organometallic chemistry of titanium and zirconium, we discovered that, though we could form very reactive metal–carbon bonds, they easily underwent migration to the highly electrophilic imino carbons of the ligand.[6b,e] In order to overcome this difficulty, we used lower oxidation states, namely Ti(III) and V(III), which thus rendered the imino groups less electrophilic, and this enabled us to isolate and study M–C bond functionalities.[6d] Although very different, the reversible alkyl migrations between the metal and the pyrrolic nitrogen have been observed in cobalt- and iron-porphyrin chemistry.[10] The second major problem we encountered with this chemistry was the stereochemistry that the tetradentate ligand imposes on the metal,[6] generating two functionalizable metal sites *trans* to each other, an undesirable characteristic for driving metal-assisted intramolecular transformations. The tetradentate Schiff bases adapted, however, to larger metals, *i.e.* Zr and Hf ions, making available *cis* reactive sites.[6c] Therefore, the dibenzotetramethyltetraaza[14]annulene dianion was used as an ancillary ligand in order to solve the stereochemical problem, since its saddle shape conformation forces the available metal-based orbitals to adopt a *cis* conformation.[7,11]

As we briefly communicated years ago,[7b] the tmtaa did not solve the problems caused by the presence on the ligand of electrophilic sites competing with the metal. A complete analysis of the [Zr(tmtaa)] fragment is reported herein, both from an experimental and theoretical approach. This will shed light on a number of facts: (i) the problems related to the generation of the ZrR_2 unit from the readily available [Zr(tmtaa)Cl_2],[7e] (ii) the conditions under which the thermal- or nucleophilic-induced alkyl migration to the ligand tmtaa can occur or not, (iii) the generation of novel forms of tmtaa-derived macrocycles, (iv) the migration of two benzyl groups to Bu^{t}NC leading to the

(2) Schwartz, J.; Labinger, J. A. *Angew. Chem., Int. Ed. Engl.* **1976**, *15*, 333. Carr, D. B.; Yoshifuji, M.; Shoer, L. I.; Gell, K. I.; Schwartz, J. *Ann. N. Y. Acad. Sci.* **1977**, *295*, 127. Neghishi, E.; Yoshida, T. *Tetrahedron Lett.* **1980**, *21*, 1501. Neghishi, E.; Takahashi, T. *Aldrichimica Acta* **1985**, *18*, 31. Neghishi, E.; Miller, J. A.; Yoshida, T. *Tetrahedron Lett.* **1984**, *25*, 3407. Jordan, R. F.; Lapointe, R. E.; Bradley, P. K.; Baenzinger, N. *Organometallics* **1989**, *8*, 2892 and references therein. Schwartz, J. *Pure Appl. Chem.* **1980**, *52*, 733. Buchwald, S. L.; La Maire, S. J.; Nielsen, R. B.; Watson, B. T.; King, S. M. *Tetrahedron Lett.* **1987**, *28*, 3895.

(3) See: *Comprehensive Organometallic Chemistry*; Wilkinson, G., Stone, F. G. A., Abel, E. W., Eds.; Pergamon: Oxford, 1982; Vol. 3.

(4) (a) Chisholm, M. H.; Rothwell, I. P. In *Comprehensive Coordination Chemistry*; Wilkinson, G., Gillard, R. D., McCleverty, J. A., Eds.; Pergamon: Oxford, 1988; Vol. 2, Chapter 15.3. (b) Chamberlain, L. R.; Durfee, L. D.; Fau, P. E.; Fanwick, P. E.; Kobriger, L.; Latesky, S. L.; McMullen, A. K.; Rothwell, I. P.; Folting, K.; Huffman, J. C.; Streib, W. E.; Wang, R. *J. Am. Chem. Soc.* **1987**, *109*, 390, 6068, and references therein. Durfee, L. D.; Fanwick, P. E.; Rothwell, I. P.; Folting, K.; Huffman, J. C. *J. Am. Chem. Soc.* **1987**, *109*, 4720. (c) Zambrano, C. H.; Fanwick, P. E.; Rothwell, I. P. *Organometallics* **1994**, *13*, 1174. (d) Hill, J. E.; Bailich, G.; Fanwick, P. E.; Rothwell, I. P. *Organometallics* **1993**, *12*, 2911. (e) Bailich, G.; Fanwick, P. E.; Rothwell, I. P. *J. Am. Chem. Soc.* **1993**, *115*, 1581. (f) Hill, J. E.; Bailich, G.; Fanwick, P. E.; Rothwell, I. P. *Organometallics* **1991**, *10*, 3428. (g) Lubben, T. V.; Wolczanski, P. T. *J. Am. Chem. Soc.* **1987**, *109*, 424 and references therein. (h) Floriani, C.; Corazza, F.; Lesueur, W.; Chiesi-Villa, A.; Guastini, C. *Angew. Chem., Int. Ed. Engl.* **1989**, *28*, 66.

(5) Collman, J. P.; Hegedus, L. S.; Norton, J. R.; Finke, R. G. *Principles and Applications of Organotransition Metal Chemistry*; University Science Books: Mill Valley, CA, 1987.

(6) (a) Gambarotta, S.; Mazzanti, M.; Floriani, C.; Chiesi-Villa, A.; Guastini, C. *J. Chem. Soc., Chem. Commun.* **1985**, 829. (b) Floriani, C.; Solari, E.; Corazza, F.; Chiesi-Villa, A.; Guastini, C. *Angew. Chem., Int. Ed. Engl.* **1989**, *28*, 64. (c) Corazza, F.; Solari, E.; Floriani, C.; Chiesi-Villa, A.; Guastini, C. *J. Chem. Soc., Dalton Trans.* **1990**, 1335. (d) Rosset, J.-M.; Floriani, C.; Mazzanti, M.; Chiesi-Villa, A.; Guastini, C. *Inorg. Chem.* **1990**, *29*, 3991. (e) Solari, E.; Floriani, C.; Chiesi-Villa, A.; Rizzoli, C. *J. Chem. Soc., Dalton Trans.* **1992**, 367.

(7) (a) Ciurli, S.; Floriani, C.; Chiesi-Villa, A.; Guastini, C. *J. Chem. Soc., Chem. Commun.* **1986**, 1401. (b) Floriani, C.; Ciurli, S.; Chiesi-Villa, A.; Guastini, C. *Angew. Chem., Int. Ed. Engl.* **1987**, *26*, 70. (c) Floriani, C.; Mazzanti, M.; Ciurli, S.; Chiesi-Villa, A.; Guastini, C. *J. Chem. Soc., Dalton Trans.* **1988**, 1361. (d) Solari, E.; De Angelis, S.; Floriani, C.; Chiesi-Villa, A.; Rizzoli, C. *Inorg. Chem.* **1992**, *31*, 96. (e) De Angelis, S.; Solari, E.; Gallo, E.; Floriani, C.; Chiesi-Villa, A.; Rizzoli, C. *Inorg. Chem.* **1992**, *31*, 2520. (f) Giannini, L.; Solari, E.; Floriani, C.; Chiesi-Villa, A.; Rizzoli, C. *Angew. Chem., Int. Ed. Engl.* **1994**, *33*, 2204. (g) Uhrhammer, R.; Black, D. G.; Gardner, T. G.; Olsen, J. D.; Jordan, R. F. *J. Am. Chem. Soc.* **1993**, *115*, 8493. (h) Goedken, V. L.; Ladd, J. A. *J. Chem. Soc., Chem. Commun.* **1981**, 910; **1982**, 142. Housmekerides, C. E.; Pilato, R. S.; Geoffroy, G. L.; Rheingold, A. L. *J. Chem. Soc., Chem. Commun.* **1991**, 563. Yang, C. H.; Ladd, J. A.; Goedken, V. L. *J. Coord. Chem.* **1988**, *18*, 317. (i) Floriani, C. *Polyhedron* **1989**, *8*, 1717.

(8) (a) Dawson, D. Y.; Brand, H.; Arnold, J. *J. Am. Chem. Soc.* **1994**, *116*, 9797. (b) Brand, H.; Arnold, J. *Angew. Chem., Int. Ed. Engl.* **1994**, *33*, 95. (c) Arnold, J.; Hoffman, C. G.; Dawson, D. Y.; Hollander, F. J. *Organometallics* **1993**, *12*, 3645. (d) Brand, H.; Arnold, J. *Organometallics* **1993**, *12*, 3655. (e) Martin, P. C.; Arnold, J.; Bocian, D. F. *J. Phys. Chem.* **1993**, *97*, 1332. (f) Kim, H.-J.; Whang, D.; Kim, K.; Do, Y. *Inorg. Chem.* **1993**, *32*, 360. (g) Arnold, J.; Johnson, S. E.; Knobler, C. B.; Hawthorne, M. F. *J. Am. Chem. Soc.* **1992**, *114*, 3996. (h) Brand, H.; Arnold, J. *J. Am. Chem. Soc.* **1992**, *114*, 2266. (i) Shibata, K.; Aida, T.; Inoue, S. *Chem. Lett.* **1992**, 1173. (j) Schavarien, C. J.; Orpen, A. G. *Inorg. Chem.* **1991**, *30*, 4968. (k) Arnold, J.; Hoffman, C. G. *J. Am. Chem. Soc.* **1990**, *112*, 8620.

(9) (a) Jacoby, D.; Floriani, C.; Chiesi-Villa, A.; Rizzoli, C. *J. Chem. Soc., Chem. Commun.* **1991**, 790. (b) Jacoby, D.; Floriani, C.; Chiesi-Villa, A.; Rizzoli, C. *J. Am. Chem. Soc.* **1993**, *115*, 3595. (c) Jacoby, D.; Floriani, C.; Chiesi-Villa, A.; Rizzoli, C. *J. Am. Chem. Soc.* **1993**, *115*, 7025. (d) Rosa, A.; Ricciardi, G.; Rosi, M.; Sgamellotti, A.; Floriani, C. *J. Chem. Soc., Dalton Trans.* **1993**, 3759. (e) Solari, E.; Musso, F.; Floriani, C.; Chiesi-Villa, A.; Rizzoli, C. *J. Chem. Soc., Dalton Trans.* **1994**, 2015.

(10) Brothers, P. J.; Collman, J. P. *Acc. Chem. Res.* **1986**, *19*, 209.

(11) (a) Cotton, F. A.; Czuchajowska, J.; Feng, X. *Inorg. Chem.* **1990**, *29*, 4329 and references therein. (b) Cotton, F. A.; Czuchajowska, J.; Falvello, L. R.; Feng, X. *Inorg. Chim. Acta* **1990**, *172*, 135. (c) Mandon, D.; Giraudon, J.-M.; Troupet, L.; Sala-Pala, J.; Guerchais, J.-E. *J. Am. Chem. Soc.* **1987**, *109*, 3490. Giraudon, J.-M.; Mandon, D.; Sala-Pala, J.; Guerchais, J.-E.; Kerbaol, J.-M.; Le Mest, Y.; L'Haridon, P. *Inorg. Chem.* **1990**, *29*, 707. Giraudon, J.-M.; Guerchais, J.-E.; Sala-Pala, J.; Troupet, L. *J. Chem. Soc., Chem. Commun.* **1988**, 921. Cotton, F. A.; Czuchajowska, J. *Polyhedron* **1990**, *21*, 2553. Housmekerides, C. E.; Ramage, D. L.; Kretz, C. M.; Shontz, J. T.; Pilato, R. S.; Geoffroy, G. L.; Rheingold, A. L.; Haggerty, B. S. *Inorg. Chem.* **1992**, *31*, 4453. Dunn, S. C.; Batsanov, A. S.; Mountford, P. *J. Chem. Soc., Chem. Commun.* **1994**, 2007. Cotton, F. A.; Czuchajowska, J. *Polyhedron* **1990**, *9*, 1221. Kuchta, M. C.; Parkin, G. *J. Am. Chem. Soc.* **1994**, *116*, 8372.

Scheme 1

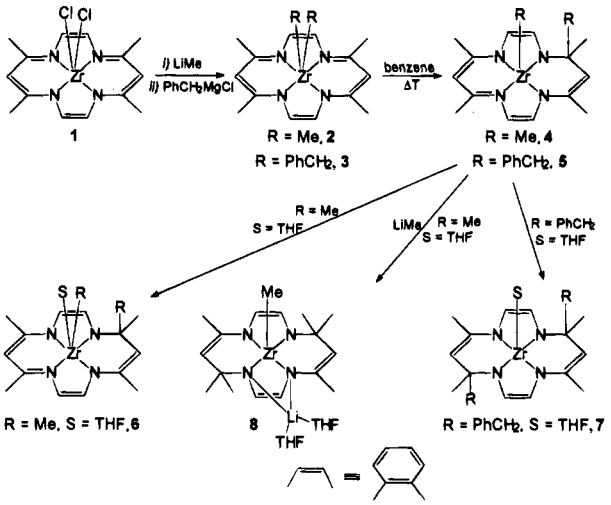

formation of a bis(η^2-iminoacyl) proving the presence on the metal of four low-lying *d* orbitals, as predicted by theory, and (v) the reaction of [Zr(tmtaa)(CH_2Ph)$_2$] with carbon monoxide, a reaction pathway which illustrates the reactivity of both the zirconium and the iminato carbon in the $[Zr(tmtaa)]^{2+}$ fragment. Some preliminary results on the chemistry and structure of two alkyl derivatives have been briefly communicated years ago.[7b]

Results and Discussion

Alkylation of [Zr(tmtaa)Cl$_2$]. The dialkyl Zr(tmtaa) compounds **2** and **3** were prepared by the metathesis reaction of **1** with the corresponding Grignard or Li reagent in melting benzene suspensions (Scheme 1).

Various problems made the successful isolation of these dialkyl derivatives in a pure form a synthetic challenge, namely: (a) when the Grignard reagent MgBzCl is used, the precipitation of Mg salts is not complete in the reaction mixture, even in the presence of excess dioxane. Removing volatiles *in vacuo* and extracting the residue with hot benzene afforded, by concentrating and cooling the resulting benzene solution, analytically pure, microcrystalline **3** in good yields. (b) In the case of the reaction with MeLi, the alkylating agent must be added very slowly and in a very accurate stoichiometry to the melting suspension of **1** in benzene; in fact, MeLi rapidly and irreversibly reacts with **3** to give a Li-containing product, later identified as **8** (*vide infra*). (c) Both alkyl species are thermally labile at room temperature (or above) in benzene solution and transform into the new products, **4** and **5** (Scheme 1). Luckily, in both cases **4** and **5** are much more soluble than the nonmigrated dialkyls, which allowed isolation of **3** free of **5** by crystallization in benzene and **2** free of **4** by washing the crude product with hexane (crystallization was discouraged by the higher thermal lability). This alkyl lability is associated with the electrophilicity of the imino groups adjacent to the M−C bonds, the electrophilicity of the imino groups being affected strongly by the oxidation state of the metal. The use of lower oxidation states for titanium and vanadium reduces the electrophilic activation of the imino group, both in Schiff bases[6d] and in tmtaa[7d] complexes, and thus allowed isolation of stable σ-bonded organometallic derivatives. Complexes **2** and **3** have been characterized by the conventional analytical methods, and they do not show any unexpected peculiarity (see the Experimental Section). The X-ray analysis of **3** exemplifies a typical structure of a dialkyl derivative (Figure 1). Selected bond distances and angles are quoted in Table 2.

The complex molecule shows a crystallographically imposed C_s symmetry, the mirror plane running through the zirconium

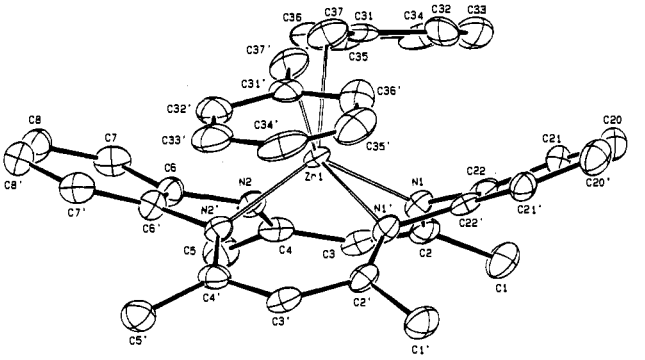

Figure 1. ORTEP drawing for complex **3** (30% probability ellipsoids). Prime refers to a transformation of *x*, *0.5* − *y*, *z*.

atom and the midpoints of the C6−C6′ and C22−C22′ bonds. The benzyl groups are η^1-bonded to the metals and *cis* to each other to form a C37−Zr1−C37′ angle of 80.2(4)°. The Zr−C bond distance [2.371(1) Å] is particularly long, as is usually found in the case of sterically-demanding substituents. The zirconium atom lies 1.017(2) Å above the N_4 core, which is rigorously planar for symmetry requirements (a similar displacement is observed in **1**). The tmtaa ligand is in the usual saddle-shaped conformation (Table 3), the zirconium atom occupying the cavity provided by the two bent aromatic rings. The five-membered chelation rings are folded along the N···N lines (Table 3), and the zirconium is displaced by 1.348(2) and 1.339(2) Å from the mean plane through N1,C22,C22′,N1′ and N2,C6,C6′,N2′, respectively. The one independent six-membered chelation ring is slightly folded along the N1···N2 line (Table 3). The two symmetry-related phenyl rings of the benzyl group are mutually oriented to form a dihedral angle of 21.1(3)° and are nearly parallel to the N_4 plane [dihedral angle 10.6(3)°]. The sequence of bond distances within the [Zr(tmtaa)] moiety is quite similar to that of **1**.[7e]

The problems encountered in the preparation of the dialkyl compounds prompted us to investigate the migratory aptitude of the Zr−C functionality in **2** and **3**.

Thermally-Induced Migrations. Both **2** and **3** are thermally and photochemically stable in the solid state in an inert atmosphere, but in benzene solutions they undergo a thermally-induced migration of one of the two alkyl groups to one of the imino carbons of the tmtaa ligand (see Scheme 1), forming **4** and **5**, respectively. The migratory aptitude depends mainly on the nature of the alkyl group. The reaction, which can be easily monitored by ^{1}H NMR spectroscopy, takes one day at room temperature for converting **2** to **4**, while **3** transforms to **5** in 6−8 h in refluxing benzene. The latter reaction takes weeks at room temperature. The alkyl migration to the tmtaa ligand transforms it into a trianionic macrocycle.

Both reactions were performed on a preparative scale with reasonable yields, limited mainly by the high solubility of the products. The proposed structure of **4** and **5** is fully consistent with the analytical and spectroscopic data. An X-ray analysis has been performed on crystals of **6**, obtained from the solvation of **4** with THF. The THF is only weakly bound, in fact it appears only slightly affected in the ^{1}H NMR spectrum recorded in C_6D_6. The structure of **6** is shown in Figure 2. Selected structural parameters are given in Table 4.

A comparison of the most relevant conformational parameters is reported in Table 5. The methylation of tmtaa affects largely the conformation of the [Zr(tmtaa)] moiety, as can be seen from the structures of **1** and **3** and related [M(tmtaa)X] complexes. There is a significant difference in the Zr−N bond distances, the shortest one being to the amido nitrogen N1 [Zr1−N1,

Table 1. Experimental Data for the X-ray Diffraction Studies on Crystalline Compounds **3**, **6**, **7**, and **10**

compound	**3**	**6**	**7**	**10**
chemical formula	$C_{36}H_{36}N_4Zr$	$C_{28}H_{36}N_4OZr$	$C_{40}H_{44}N_4OZr{\cdot}2C_6H_6$	$C_{46}H_{54}N_6Zr{\cdot}C_7H_8$
a (Å)	16.028(3)	19.859(5)	23.608(6)	12.800(4)
b (Å)	20.666(4)	14.771(5)	9.529(3)	15.795(5)
c (Å)	9.018(2)	9.072(4)	19.050(4)	11.758(1)
α (deg)	90	90	90	91.8(2)
β (deg)	90	93.85(3)	99.30(2)	93.56(1)
γ (deg)	90	90	90	97.81(2)
V (Å^3)	2987.1(10)	2655.2(16)	4229.2(19)	2348.7(1)
Z	4	4	4	2
fw	615.9	535.8	842.2	874.3
space group	*Pnma* (#62)	P_1/n (#13)	*C*2/c (#15)	$P\bar{1}$ (#2)
T (°C)	22	22	−130	22
λ (Å)	0.71069	0.71069	1.54178	1.54178
ϱ_{calcd} (g cm^{-3})	1.370	1.341	1.326	1.236
μ (cm^{-1})	3.91	4.32	24.67	22.32
transmn coeff	0.694−1.000	0.967−1.000	0.713−1.000	0.875−1.000
R^a	0.063	0.044	0.046	0.042
$R_w{}^b$	0.065	0.045	0.055	0.049

^{a} $R = \sum|\Delta F|/\sum|F_o|$. ^{b} $R_w = \sum w^{1/2}|\Delta F|/\sum w^{1/2}|F_o|$.

Table 2. Selected Bond Distances (Å) and Angles (deg) for Complex **3**[a]

	Distances		
Zr1−N1	2.183(8)	N2−C6	1.437(13)
Zr1−N2	2.193(8)	C2−C3	1.400(17)
Zr1−C37	2.371(13)	C3−C4	1.436(16)
N1−C2	1.324(14)	C6−C6′	1.409(15)
N1−C22	1.416(15)	C22−C22′	1.418(15)
N2−C4	1.307(13)		
	Angles		
C37−Zr1−C37′	80.2(4)	N1−C2−C1	123.1(10)
N2−Zr1−C37	87.4(4)	C1−C2−C3	113.7(9)
N2−Zr1−N2′	72.7(3)	N1−C2−C3	123.0(10)
N1−Zr1−C37	89.8(4)	C2−C3−C4	129.6(10)
N1−Zr1−N1′	71.9(3)	N2−C4−C3	121.5(10)
N1−Zr1−N2	82.6(3)	C3−C4−C5	114.6(10)
Zr1−N1−C22	104.0(6)	N2−C4−C5	123.8(10)
Zr1−N1−C2	130.5(7)	N2−C6−C7	125.1(9)
C2−N1−C22	125.1(9)	N2−C6−C6′	114.5(9)
Zr1−N2−C6	103.4(6)	N1−C22−C21	126.9(9)
Zr1−N2−C4	131.3(7)	N1−C22−C22′	113.8(10)
C4−N2−C6	124.7(8)	Zr1−C37−C31	121.0(8)

[a] ′ denotes x, 0.5 − y, z.

Table 3. Comparison of Structural Parameters for Complexes **3** and **10**[a]

complex		**3**	**10**
dist of atoms from the N_4 core (Å)	N1	0.000(8)	−0.124(3)
	N2	0.000(8)	0.124(3)
	N3		−0.122(3)
	N4		0.123(3)
	Zr1	1.017(2)	1.265(1)
folding[b] along the N1···N2 line (deg)		9.1(3)	8.3(1)
folding along the N2···N3 line (deg)		52.4(2)	54.0(1)
folding along the N3···N4 line (deg)		9.1(3)	8.4(1)
folding along the N1···N4 line (deg)		52.7(2)	53.8(1)
angle between the N1,C_3,N2 and N3,C_3,N4 planes (deg)		58.2(4)	72.7(1)
angle between the N1,C_6,N4 and N2,C_6,N3 planes (deg)		34.8(2)	28.5(1)
dist of Zr1 from the N1,C_3,N2 plane (Å)		0.261(2)	0.266(1)
distof Zr1 from the N3,C_3,N4 plane (Å)		0.261(2)	0.270(1)
dist of Zr1 from the N1,C_6,N4 plane (Å)		1.422(2)	1.570(1)
dist of Zr1 from the N2,C_6,N3 plane (Å)		1.419(2)	1.575(1)

[a] N1,C_3,N2; N3,C_3,N4; N1,C_6,N4; and N2,C_6,N3 define the planes through atoms N1,C2,C3,C4,N2; N3,C13,C14,C15,N4; N1,C22, C21,C20,C19,C18,C17,N4; and N2,C6,C7,C8,C9,C10,C11,N3, respectively. In complex **6** the atoms N3, N4, C9, C10, C11, C13, C14, C15, C17, C18, C19 should be read N2′, N1′, C8′, C7′, C6′, C4′, C3′, C2′, C22′, C21′, C20′, respectively. [b] The folding is defined as the dihedral angle between the N,Zr,N and the N,C_3,N or N,C_6,N planes of a five- or six-membered chelation ring, respectively.

2.128(5) Å]. The alkylation causes some folding of half of the tmtaa ligand, causing a sort of Zr−allyl interaction with the C3−C4−N2 fragment [Zr−azaallyl(centroid), 2.292(7) Å], though the dihedral angle between the Zr−azallyl direction and the azaallyl plane [49.4(6)°] does not truly support such a description.

The C24−Zr1−O1 plane is nearly perpendicular to the N_4 core [dihedral angle 86.2(1)°], is parallel to the N1−N2 and N3−N4 vectors, and is perpendicular to the N1−N4 and N2−N3 vectors. The cavity in which the Zr−X_2 is located is similar to that defined by two cyclopentadienyl rings in the [cp_2ZrX_2] series[1c] and is provided by the bending of the acetylacetoniminato residues. This conformation is completely different from that observed in **1**, **3**, and [M(tmtaa)X],[7d] where the cavity is provided by the bending of the aromatic ring and the ZrX_2 plane is perpendicular to the N1−N2 and N3−N4 vectors.

The positioning of the Zr atom in the cavity formed by the bending of the acetylacetoniminato moieties rather than in the cavity formed by the aromatic rings causes other significant structural differences between the alkylated and nonalkylated complexes concerning the conformation of the five- and six-membered chelation rings (Tables 5 and 8). The five-membered chelation rings are approximately planar, the maximum displacements being 0.0246(6) Å for C22 in the Zr1,N1,C22,C17,-

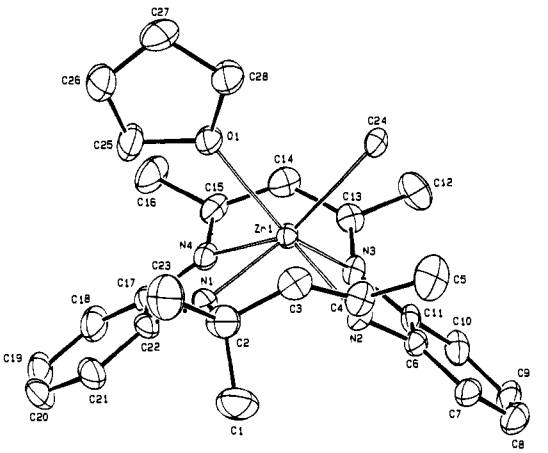

Figure 2. ORTEP drawing for complex **6** (30% probability ellipsoids).

N4 ring and 0.089(6) Å for C6 in the Zr1,N2,C6,C11,N3 ring, with the zirconium lying on both of these planes. The six-membered chelation rings are folded with respect to the N···N

Table 4. Selected Interatomic Distances (Å) and Angles (deg) for Complex **6**

		Distances	
Zr1−O1	2.386(5)	N2−C6	1.387(7)
Zr1−N1	2.128(5)	N3−C11	1.405(8)
Zr1−N2	2.135(5)	N3−C13	1.332(9)
Zr1−N3	2.188(5)	N4−C15	1.320(10)
Zr1−N4	2.191(4)	N4−C17	1.400(8)
Zr1−C3	2.681(8)	C1−C2	1.5688(12)
Zr1−C4	2.653(7)	C2−C3	1.542(11)
Zr1−C24	2.418(6)	C2−C23	1.573(12)
O1−C25	1.452(9)	C3−C4	1.362(10)
O1−C28	1.454(9)	C6−C11	1.407(9)
N1−C2	1.430(10)	C13−C14	1.415(9)
N1−C22	1.383(8)	C14−C15	1.412(9)
N2−C4	1.361(8)	C17−C22	1.422(10)
		Angles	
N3−Zr1−C24	88.0(2)	C1−C2−C23	109.6(7)
N3−Zr1−N4	77.8(2)	C1−C2−C3	107.5(7)
N2−Zr1−C24	92.4(2)	N1−C2−C23	113.2(7)
N2−Zr1−N3	70.7(2)	N1−C2−C3	107.2(6)
N1−Zr1−N4	71.5(2)	C3−C2−C23	106.6(6)
N1−Zr1−N2	85.2(2)	C2−C3−C4	124.2(7)
O1−Zr1−C24	80.3(2)	N2−C4−C3	116.9(6)
O1−Zr1−N4	84.0(1)	C3−C4−C5	121.4(7)
O1−Zr1−N1	83.6(2)	N2−C4−C5	119.8(6)
Zr1−O1−C28	126.5(4)	N2−C6−C11	112.2(5)
Zr1−O1−C25	124.7(4)	N2−C6−C7	127.4(6)
C25−O1−C28	107.4(5)	N3−C11−C10	126.8(6)
Zr1−N1−C22	122.6(4)	N3−C11−C6	113.8(5)
Zr1−N1−C2	110.3(4)	N3−C13−C12	122.9(6)
C2−N1−C22	126.6(6)	C12−C13−C14	117.4(6)
Zr1−N2−C6	122.8(4)	N3−C13−C14	119.4(6)
Zr1−N2−C4	96.2(4)	C13−C14−C15	126.4(7)
C4−N2−C6	129.7(5)	N4−C15−C14	119.5(6)
Zr1−N3−C13	106.3(4)	C14−C15−C16	116.6(7)
Zr1−N3−C11	119.5(4)	N4−C15−C16	123.6(6)
C11−N3−C13	127.9(5)	N4−C17−C22	113.6(5)
Zr1−N4−C17	119.2(4)	N4−C17−C18	125.2(7)
Zr1−N4−C15	108.1(4)	N1−C22−C21	128.1(6)
C15−N4−C17	130.0(5)	N1−C22−C17	113.0(6)
N1−C2−C1	112.2(6)		

Table 5. Comparison of Structural Parameters for Complexes **6** and **7**[a]

complex		**6**	**7**
dist of atoms from the N_4 core (Å)	N1	0.010(5)	0.156(3)
	N2	−0.008(5)	−0.156(3)
	N3	0.010(5)	0.156(3)
	N4	−0.010(5)	−0.156(3)
	Zr1	1.049(1)	0.874(1)
folding[b] along the N1···N2 line (deg)		72.2(2)	67.8(1)
folding along the N2···N3 line (deg)		4.7(2)	3.9(1)
folding along the N3···N4 line (deg)		67.4(2)	67.8(1)
folding along the N1···N4 line (deg)		3.9(2)	3.9(2)
angle between the N1,C_3,N2 and N3,C_3,N4 planes (deg)		59.6(2)	63.9(1)
angle between the N1,C_6,N4 and N2,C_6,N3 planes (deg)		72.7(1)	57.1(1)
dist of Zr1 from the N1,C_3,N2 plane (Å)		1.529(1)	1.430(1)
distof Zr1 from the N3,C_3,N4 plane (Å)		1.588(1)	1.430(1)
dist of Zr1 from the N1,C_6,N4 plane (Å)		0.131(1)	0.057(1)
dist of Zr1 from the N2,C_6,N3 plane (Å)		0.118(1)	0.057(1)

[a] N1,C_3,N2; N3,C_3,N4; N1,C_6,N4; and N2,C_6,N3 define the planes through atoms N1,C2,C3,C4,N2; N3,C13,C14,C15,N4; N1,C22,C21, C20,C19,C18,C17,N4; and N2,C6,C7,C8,C9,C10,C11,N3, respectively. In complex **6** the atoms N3, C13, C14, C15, N4, C17, C18, C19, C20, C21, C22 should be read N1′, C2′, C3′, C4′, N2′, C6′, C7′, C8′, C9′, C10′, C11′, respectively. [b] The folding is defined as the dihedral angle between the N,Zr,N and the N,C_3,N or N,C_6,N planes of a five- or six-membered chelation ring, respectively.

line (Table 5), Zr1 being displaced by 1.529(1) and 1.588(1) Å from the mean planes through N1,C_3,N2 and N3,C_3, N4, respectively. The N3−C13−C14−C15−N4 chain is nearly planar (maximum displacements from the mean plane ranging from −0.467(8) to 0.215(7) Å for C2 and C3, respectively).

Table 6. Selected Interatomic Distances (Å) and Angles (deg) for Complex **7**[a]

		Distances	
Zr1−O1	2.238(3)	N2−C6	1.404(3)
Zr1−N1	2.130(3)	C2−C3	1.536(4)
Zr1−N2	2.151(2)	C2−C23	1.554(4)
Zr1−C3	2.681(4)	C3−C4	1.375(3)
Zr1−C4	2.591(4)	C6−C11	1.426(5)
N1−C2	1.479(4)	N2−C4	1.374(4)
N1−C11′	1.389(4)		
		Angles	
N2−Zr1−N1′	71.0(1)	C1−C2−C3	110.7(3)
N1−Zr1−N2	90.2(1)	N1−C2−C23	114.9(3)
O1−Zr1−N2	118.6(1)	N1−C2−C3	105.3(3)
O1−Zr1−N1	109.7(1)	C3−C2−C23	107.4(2)
Zr1−N1−C11′	122.9(2)	C2−C3−C4	127.0(3)
Zr1−N1−C2	109.4(2)	N2−C4−C3	117.7(3)
C2−N1−C11′	125.7(2)	C3−C4−C5	120.5(3)
Zr1−N2−C6	121.1(2)	N2−C4−C5	121.0(2)
Zr1−N2−C4	91.9(2)	N2−C6−C11	112.3(3)
C4−N2−C6	125.2(3)	N2−C6−C7	126.4(3)
N1−C2−C1	110.9(3)	N1′−C11−C6	111.9(3)
C1−C2−C23	107.5(2)	N1′−C11−C10	130.5(3)
		C2−C23−C13	116.9(2)

[a] ′ denotes $-x$, y, $-0.5 - z$.

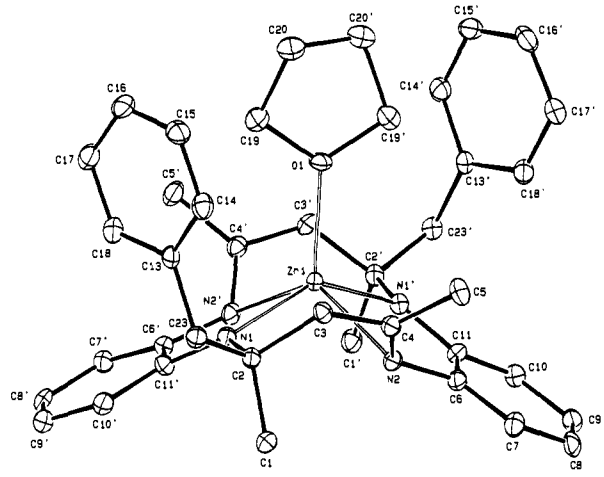

Figure 3. ORTEP drawing for complex **7** (30% probability ellipsoids). Prime refers to a transformation of $-x$, y, $-0.5 - z$.

Ligand-Induced Migrations. Compound **5** is stable in refluxing benzene for days, but in coordinating solvents a further migration process occurs which involves the second Zr−R functionality (Scheme 1).

In THF the transformation requires refluxing overnight to be complete; the product **7** is crystallized from benzene in good yields (see Experimental Section) and has been fully characterized, including an X-ray analysis (*vide infra*).

The migration of the second alkyl occurs also at room temperature, assisted by the more nucleophilic pyridine solvent.

The migration of the second benzyl group to the remaining imino functionality in the macrocycle leads to the formation of a tetraanionic amido macrocyclic ligand. The structure has been disclosed by an X-ray analysis on **7** (Figure 3). The structure consists of discrete monomers and benzene solvent molecules of crystallization in the complex/solvent molar ratio of 1/2. Selected bond distances and angles are given in Table 6.

The complex possesses a crystallographically imposed *C*2 symmetry, the twofold axis running through the Zr1−O1 bond. Coordination around the zirconium atom is a distorted square-pyramid with the N_4 core showing remarkable tetrahedral

distortions (Table 5), the zirconium being displaced by 0.874(1) Å. The Zr1−O1 line is exactly perpendicuar to the N_4 core, as dictated by symmetry requirements. The benzylic phenyl rings lie perpendicular to the N_4 core [dihedral angle 85.6(2)°], being nearly parallel to each other [dihedral angle 8.8°]. In analogy with complex **6**, the two symmetry-related five-membered chelation rings are planar [maximum out-of-plane distance 0.061(3) Å for C6]; the zirconium atom again lies on both of these planes. The double alkylation greatly increases the four C−N bond distances, especially N1−C2 [1.479(4) Å] and to a lesser extent N2−C4 [1.374(4) Å], which approach the length of a C−N single bond. As for complex **6**, the alkylation causes the loss of planarity in the six-membered chelation rings and thus the folding of the formerly planar $N1C_3N2$ chains. The two C3−C4−N2 fragments approach the metal in pseudoazaallyl forms [Zr−azaallyl(centroid), 2.268(4) Å; dihedral angle between the Zr−centroid direction and the azaallyl plane 42.0(2)°]. The overall geometry of the macroring is therefore similar to that observed in complex **6**, with the zirconium lying in the cavity provided by the acetylacetoniminato residues. The conformational parameters of the novel ligand are listed in Table 5.

Complex **4** shows a migratory aptitude of the second alkyl group significantly different from that for **5**. It is quite stable even in refluxing THF (unidentified byproducts begin to form over a period of hours), but both **2** and **4** readily react with a strong nucleophile such as MeLi in benzene solutions to give **8**. This reaction involves the migration of both methyl groups from zirconium to the imino carbons, with a further alkylation by LiMe at the metal. Thus we have discovered that complex **8** can be easily prepared from an exhaustive methylation of **1** with 3 equiv of LiMe. Complex **8** has been fully characterized including an X-ray analysis showing the ion-pair form of **8**, having the lithium cation attached to the periphery of the macrocycle.[12]

The particular lability of the Zr−C bond in complexes **2**−**5** has been observed in terms of the intramolecular migration of the alkyl groups from the metal to the ligand. A major question arises at this point, concerning the intra- or intermolecular nature of the alkyl migration mechanism. The two processes are extremely selective. The absence of any mixture of compounds derived from the mono- and dimigration at the same time is very much in favor of an intramolecular process. An intermolecular alkyl transfer, however, cannot be excluded, and in fact we found that an alkyl exchange process can easily take place between **1** and **3** both in CH_2Cl_2 and in C_6H_6 (Scheme 2). Such an equilibrium gives rise to a mixture of **1**, **3**, and **9**. Complex **9** might not be isolated free of **3** and **1** either from the redistribution reaction between **1** and **3** or by the alkylation of **1** with the appropriate 1:1 stoichiometry (see Experimental Section). In such a case, however, the alkyl transfer pathway is very much different. The structures of the $[Zr(tmtaa)_2]$[7e] and **10**, where zirconium achieves the octacoordination, along with the existence of four low lying d-orbitals on the metal, prompt us to suggest the intermediacy of alkyl- and chloro-bridged dimetallic species, such as A, in the alkyl transfer leading to the equilibrium shown in Scheme 2.

Alkyl Migration to an Incoming Substrate: Reactions with Bu^{t}NC and CO. The best candidate for studying the migratory insertion of Zr alkyls[13] with incoming substrates is **3** because of its relatively high thermal inertness, compared to those of the other alkyl derivatives so far mentioned in this series. The reaction of **3** with Bu^{t}NC in toluene carried out as reported in detail in the Experimental Section proceeds as shown in Scheme 3 and leads to **10**. The precoordination of isocyanides by **3** is quite feasible, since in tmtaa complexes zirconium can expand its coordination sphere up to coordination number 8, as in $[Zr(tmtaa)_2]$ and complex **10**.[7e]

The formation of η^2-iminoacyls is quite a common reaction in the organometallic chemistry of zirconium,[13,14] though rather

Scheme 2

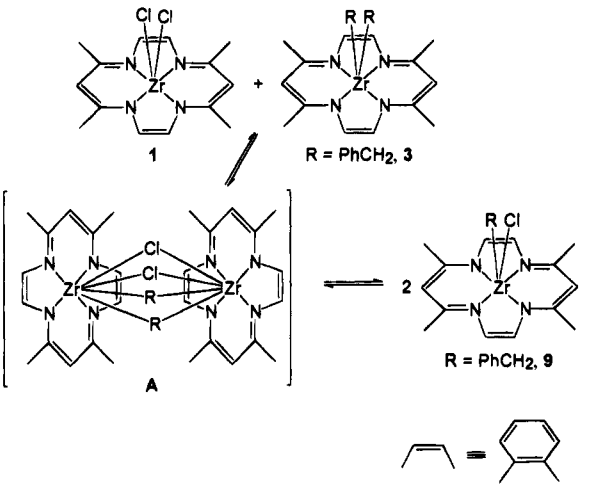

Scheme 3

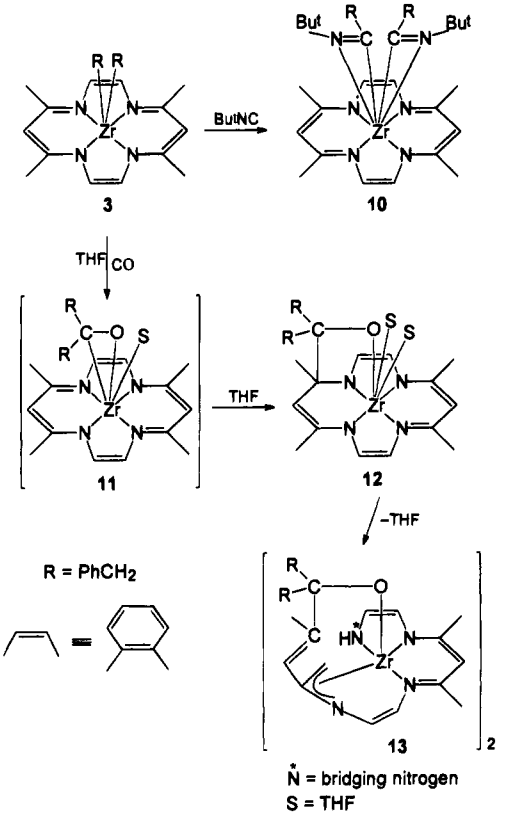

(12) Giannini, L.; Solari, E.; Floriani, C.; Chiesi-Villa, A.; Rizzoli, C. Unpublished results.

(13) Durfee, L. D.; Rothwell, I. P. *Chem. Rev.* **1988**, *88*, 1059.

(14) Iminoacyl formed from migratory insertion of RNC with M−C bonds is a well-known reaction: Singleton, E.; Ossthnizen, H. E. *Adv. Organomet. Chem.* **1983**, *22*, 209. Otsuka, S.; Nakamura, A.; Yoshida, T.; Naruto, M.; Ataba, K. *J. Am. Chem. Soc.* **1973**, *95*, 3180. Yamamoto, Y.; Yamazaki, H. *Inorg. Chem.* **1974**, *13*, 438. Aoki, K.; Yamamoto, Y. *Inorg. Chem.* **1976**, *15*, 48. Bellachioma, G.; Cardaci, G.; Zanazzi, P. *Inorg. Chem.* **1987**, *26*, 84. Maitlis, P. M.; Espinet, P.; Russell, M. J. H. In *Comprehensive Organometallic Chemistry*; Wilkinson, G., Stone, F. G. A., Abel, E. W., Eds.; Pergamon: London, 1982; Vol. 8, Chapter 38.4. Crociani, B. In *Reactions of Coordinated Ligands*; Braterman, P. S., Ed.; Plenum: New York, 1986; Chapter 9.

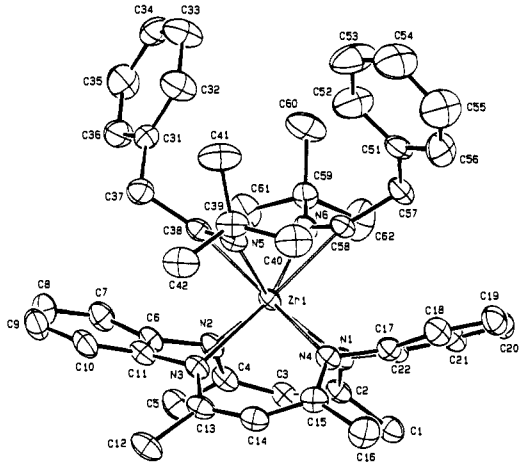

Figure 4. ORTEP drawing for complex **10** (30% probability ellipsoids).

less examples document the formation of a bis(η^2-iminoacyl).[15] This reaction is normally concurrent with the migration of both alkyl groups to the same isocyanide, as is observed in the analogous reaction of **3** with carbon monoxide. In the case of isocyanide it proceeds to a much lesser extent because of the lower carbenium ion nature of the carbon in the η^2-iminoacyl.[16] The structure of **10** is shown in Figure 4. The structure consists of discrete monomers and toluene solvent molecules of crystallization in the complex/solvent molar ratio of 1/1. Selected bond distances and angles are given in Table 7.

The zirconium metal is σ-bonded to the nitrogens of the N_4 plane and η^2-N,C bonded to the iminoacyl groups. The asymmetry and the lengthening of the Zr−N bond distances can be ascribed to the increased steric hindrance of the iminoacyl groups which forces zirconium out of the N_4 plane [1.265(1) Å]. The insertion of isocyanide groups into the Zr−C bonds does not much affect the conformation of the tmtaa ligand with respect to that of the starting compound; *i.e.*, the folding of the five- and six-membered chelation rings resembles that observed in complex **3**. The main difference involves the mutual orientation of the opposite NC_3N planes which form a dihedral angle of 72.7(1)° as a consequence of the steric interactions with the overlapping Bu^t groups. The dihedral angle formed by the Zr1,N5,C38 and Zr1,N6,C58 planes is 88.2(2)°. Bond distances and angles within the tmtaa ligand and η^2-iminoacyl do not show any unusual features.[13,14] The conformation of the tmtaa ligand in the complexes so far reported deserves a short comment. The bending between the acetylacetonato fragments varies (see Table 8) between 103.7(2)° and 121.8(4)°. The bending of the aromatic rings is affected much more by the presence of hindered ligands, varying from 107.3(1)° to 151.5(1)°.

The reaction of **3** with carbon monoxide concludes the various migration processes we have so far observed in the Zr alkyl derivatives and shows their complexity. Complex **3** reacts instantaneously with 1 mol of CO *per* Zr in THF to give a bright-red solid (**12**) in a red supernatant that contained a complex mixture of products, as determined by ^{1}H NMR. The red solid was obtained in a crystalline form by extraction with CH_2Cl_2/THF (~10/1). Dissolution of **12** in CH_2Cl_2 and prolonged standing in it gave crystals of the rather insoluble complex **13** upon complete evaporation of the solvent in the drybox.

The plausible sequence leading to **12**, then to **13**, is shown in Scheme 3. The migration of the two benzyl groups to the same CO (see **11**) accounts for the very high oxycarbene character of the intermediate η^2-acyl acting as accepting group.[13,16] The formation of an η^2-ketone in titanium and zirconium chemistry has significant precedents in cyclopentadienyl[17] and cyclooctatetraene chemistry.[18] The assistance of the solvent THF promotes the migration of the ketonic carbon to the imino carbon of tmtaa (see **12**), like in the processes outlined in the case of [Zr(tmtaa)(R)$_2$] complexes (see Scheme

Table 7. Selected Interatomic Distances (Å) and Angles (deg) for Complex **10**

		Distances	
Zr1−N1	2.345(3)	N4−C15	1.343(4)
Zr1−N2	2.284(3)	N4−C17	1.409(4)
Zr1−N3	2.361(2)	N5−C38	1.272(4)
Zr1−N4	2.286(3)	N5−C39	1.505(4)
Zr1−N5	2.220(3)	N6−C58	1.266(4)
Zr1−N6	2.217(2)	N6−C59	1.511(4)
Zr1−C38	2.264(4)	C2−C3	1.393(5)
Zr1−C58	2.280(4)	C3−C4	1.406(5)
N1−C2	1.333(5)	C6−C11	1.427(4)
N1−C22	1.416(4)	C13−C14	1.390(5)
N2−C4	1.328(5)	C14−C15	1.394(5)
N2−C6	1.417(5)	C17−C22	1.410(4)
N3−C11	1.411(5)	C37−C38	1.519(6)
N3−C13	1.321(4)	C57−C58	1.515(5)
		Angles	
N6−Zr1−C58	32.7(1)	Zr1−N6−C59	150.3(2)
N5−Zr1−C38	32.9(1)	Zr1−N6−C58	76.4(2)
N3−Zr1−N4	77.8(1)	C58−N6−C59	132.7(3)
N2−Zr1−N3	68.1(1)	C1−C2−C3	115.4(3)
N1−Zr1−N4	68.0(1)	N1−C2−C3	121.9(3)
N1−Zr1−N2	77.3(1)	C2−C3−C4	129.7(3)
Zr1−N1−C22	104.4(2)	N2−C4−C3	122.9(3)
Zr1−N1−C2	132.8(2)	N2−C6−C11	114.6(3)
C2−N1−C22	122.7(3)	N3−C11−C6	114.5(3)
Zr1−N2−C6	104.6(2)	N3−C13−C14	123.3(3)
Zr1−N2−C4	133.7(2)	C13−C14−C15	129.7(3)
C4−N2−C6	121.1(3)	N4−C15−C14	123.5(3)
Zr1−N3−C13	131.5(2)	N4−C17−C22	114.7(3)
Zr1−N3−C11	104.0(2)	N1−C22−C17	114.6(3)
C11−N3−C13	124.4(3)	N5−C38−C37	128.4(3)
Zr1−N4−C17	104.9(2)	Zr1−C38−C37	159.3(3)
Zr1−N4−C15	132.8(2)	Zr1−C38−N5	71.6(2)
C15−N4−C17	121.7(3)	N6−C58−C57	129.7(3)
Zr1−N5−C39	149.3(3)	Zr1−C58−C57	158.7(3)
Zr1−N5−C38	75.4(2)	Zr1−C58−N6	70.9(2)
C38−N5−C39	134.0(3)		

Table 8. Comparison of the Bending in the tmtaa Ligand for Some Complex Derivatives

complex	N1C$_6$N4 ∧ N2C$_6$N3	N1C$_3$N2 ∧ N3C$_3$N4
[Zr(tmtaa)Cl$_2$] (**1**)	128.4(1)	114.1
[Zr(tmtaa)(PhCH$_2$)$_2$] (**3**)	145.2(2)	121.8(4)
[Zr(tmtaa)(Me)$_2$·(THF)] (**6**)	107.3(1)	120.4(2)
[Zr(tmtaa)(PhCH$_2$)·(THF)] (**7**)	122.9(1)	116.1(1)
[Zr(tmtaa)(Bu^{t}NCCH$_2$Ph)$_2$] (**10**)	151.5(1)	107.3(1)
[Zr(tmtaa)$_2$]	148.1(1) (mean value)	103.7(2) (mean value)

(15) Chamberlain, L. R.; Durfee, L. D.; Fanwick, P. E.; Kobriger, L.; Latesky, S. L.; McMullen, A. K.; Rothwell, I. P.; Folting, K.; Huffman, J. C.; Streib, W. E.; Wang, R. *J. Am. Chem. Soc.* **1987**, *109*, 390.

(16) (a) Tatsumi, K.; Nakamura, A.; Hofmann, P.; Stauffert, P.; Hoffmann, R. *J. Am. Chem. Soc.* **1985**, *107*, 4440. (b) Martin, B. D.; Matchett, S. A.; Norton, J. R.; Anderson, O. P. *J. Am. Chem. Soc.* **1985**, *107*, 7952. (c) Fanwick, P. E.; Kobriger, L. M.; McMullen, A. K.; Rothwell, I. P. *J. Am. Chem. Soc.* **1986**, *108*, 8095. (d) Arnold, J.; Tilley, T. D.; Rheingold, A. L. *J. Am. Chem. Soc.* **1986**, *108*, 5355.

(17) Erker, G.; Dorf, U.; Czisch, P.; Petersen, J. L. *Organometallics* **1986**, *5*, 668. Rosenfeldt, F.; Erker, G. *Tetrahedron Lett.* **1980**, *21*, 1637. Erker, G. *Acc. Chem. Res.* **1984**, *17*, 103.

(18) Stella, S.; Floriani, C. *J. Chem. Soc., Chem. Commun.* **1986**, 1053. Berno, P.; Stella, S.; Floriani, C.; Chiesi-Villa, A.; Guastini, C. *J. Chem. Soc., Dalton Trans.* **1990**, 2669.

1). Then complex **12** upon long standing in CH_2Cl_2 evolves to **13**. The loss of THF and the consequent metal coordinative unsaturation may be primarly responsible for such a kind of transformation. The high basicity of the amido nitrogen enables it to deprotonate one of the peripheral methyl groups, leading to the monomeric form of **13** collapsing to a stable, rather insoluble dimer. The analytical and spectroscopic characterizations of **12** and **13** are given in the Experimental Section, while the X-ray analysis results on **13** are included in the Supplementary Material, since **13** is a structural curiosity which served essentially to elucidate the migratory pathways preferred by the [Zr(tmtaa)R_2] complexes in the presence of carbon monoxide. The alkyl migration processes in Zr tmtaa derivatives exemplifies and clarifies the major problems which have been encountered when the Zr−C bond functionality is induced to react in a rather complicated macrocyclic environment. This is certainly true in the case of Schiff bases and also porphyrin derivatives.[8d] The assistance of the ligand is crucial in promoting alkyl migration processes. The intervention of the ligand as an alkyl acceptor in competition with or subsequent to an incoming nucleophile is an interesting though complicating factor. From our modeling studies we can clearly state that the alkylation or functionalization of the tmtaa ligand passes through the assistance of the metal.

Extended Hückel Analysis. Over the years we, as well as others, have collected a number of structures and reactivity patterns for the $[Zr(tmtaa)]^{2+}$ [8] moiety which we analyze here with the extended Hückel methodology[19−21] with parameters taken from ref 16a and 22. By comparing its frontier orbitals to those of the well-known bent $[Cp_2Zr]^{2+}$ fragment,[23] we will emphasize similarities and differences between these two building blocks.

In our analysis, we simplified the tmtaa ligand by replacing the benzene by ethylene and the methyl groups by hydrogens. Cotton *et al.* used this simplified model in SCF-X_α-SW calculations and showed it correlated very well with the results obtained with the whole ligand.[11a,b] Further, the ligand geometry was optimized to C_{2v}, derived from the structure of [Zr(tmtaa)-Cl_2].[7e]

The $[Zr(tmtaa)]^{2+}$ fragment is built step by step. Let us first consider a planar ligand of D_{2h} symmetry. Its frontier orbitals are depicted in Figure 5. The circles indicate the phase relationship of the top lobe of each π-orbital. While the negative charge is located predominantly on the four nitrogens (−0.957), some deposits of negative charge are present on the β carbons (−0.283) of the iminato fragment. This charge buildup was found to be responsible for the 1,4-cycloadduct between acetylene and [Co(tmtaa)pyridine] reported by Goedken[24,25] and analyzed by Tatsumi and Hoffmann.[22] The significant positive charge on the iminato carbon (+0.383) will play a key role in our analysis.

The tmtaa ligand adopts a saddle shape conformation upon coordination. The phenylenediamine moieties bend up (22.3°) while the iminato counterparts bend down (32.2°). Upon bending, the system is stabilized and the frontier orbitals retain many of their characteristics. Upon coordination, these orbitals interact with those of zirconium, and the resulting MO diagram is presented in Figure 6. The d_{xy} orbital has a strong overlap

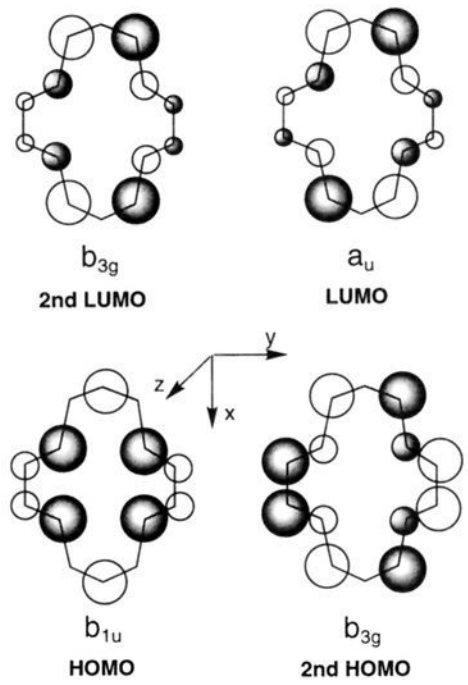

Figure 5. Frontier orbitals of the simplified $(tmtaa)^{4-}$ ligand.

with the N lone pair combinations of a_2 symmetry and, therefore, is pushed up high in energy. Due to mixing with the corresponding p orbitals and a poorer overlap with the ligand, the d_{xz} and d_{yz} orbitals are not destabilized much. With a d^0 electron count, the HOMO is the $1a_1$ orbital. The LUMO, the $2a_1$ orbital, lies 1.9 eV above. Within 1.2 eV, we find six empty orbitals, two of which are ligand-centered. For comparison, we report on the right of Figure 6 the five metal-based empty orbitals of bent $[Cp_2Zr]^{2+}$. Just as the three lowest lying empty orbitals dictate the geometry and reactivity of the $[Cp_2Zr]^{2+}$ fragment, we can qualitatively rationalize most of the structures reported to date with the help of the frontier orbitals of the $[Zr(tmtaa)]^{2+}$ fragment.

Let us consider first an hexacoordinate complex [Zr(tmtaa)-R_2]. The two σ-orbitals of the alkyl groups form in-phase and out-of-phase combinations which interact with the $2a_1$ and $2b_1$ orbitals of the metal. Such an interaction leaves the $1a_2$ orbital unperturbed (a_u orbital in Figure 5). This purely ligand-based orbital is thus the LUMO for hexacoordinate complexes. As this orbital is mostly localized on the iminato carbons, one can expect these atoms to display a marked electrophilicity. This latter is responsible for the migration of one alkyl group from the metal to the iminato carbon, probably via a mechanism similar to that presented in Schemes 2 and 3.

We now turn our attention to the metal-based empty orbitals. The four lowlying d-orbitals can accommodate up to four extra ligands. $[Zr(tmtaa)_2]$ and the bis(η^2-isonitrile) **10** are two such examples. There is, however, a delicate balance between the metal- and ligand-centered empty orbitals. An incoming nucleophile might attack either the metal or the iminato carbon. Isonitriles and carbon monoxide, which have a high metal affinity, add on to the metal.

We have simulated the approach of CO toward the [Zr(tmtaa)-Me_2], with concomitant relaxation of the methyl groups, and compare its energy profile to the approach of CO toward [$ZrCp_2$-Me_2], see Figure 7.[16a] While only a small activation barrier is observed for $[Cp_2ZrMe_2]$, followed by significant stabilization, the Walsh diagram for $[Zr(tmtaa)Me_2]$ is dramatically different. We computed a high activation barrier and an overall destabilization for the precoordination of CO to this fragment. This implies that the $[Zr(tmtaa)]^{2+}$ fragment is less electrophilic than its $[Cp_2Zr]^{2+}$ analogue.

Recently, Dronskowski and Hoffmann introduced an electrophilicity index in the extended Hückel methodology.[26,27]

(19) Hoffmann, R.; Lipscomb, W. N. *J. Chem. Phys.* **1962**, *36*, 2179.
(20) Hoffmann, R. *J. Chem. Phys.* **1963**, *39*, 1397.
(21) Ammeter, J. H.; Bürgi, H. B.; Thiebeault, J. C.; Hoffmann, R. *J. Am. Chem. Soc.* **1978**, *100*, 3686.
(22) Tatsumi, K.; Hoffmann, R. *Inorg. Chem.* **1981**, *20*, 3771.
(23) Lauher, J. W.; Hoffmann, R. *J. Am. Chem. Soc.* **1976**, *98*, 1729.
(24) Weiss, M. C.; Goedken, V. L. *J. Am. Chem. Soc.* **1976**, *98*, 3389.
(25) Weiss, M. C.; Gordon, G. C.; Goedken, V. L. *J. Am. Chem. Soc.* **1979**, *101*, 857.
(26) Dronskowski, R. *J. Am. Chem. Soc.* **1992**, *114*, 7230.

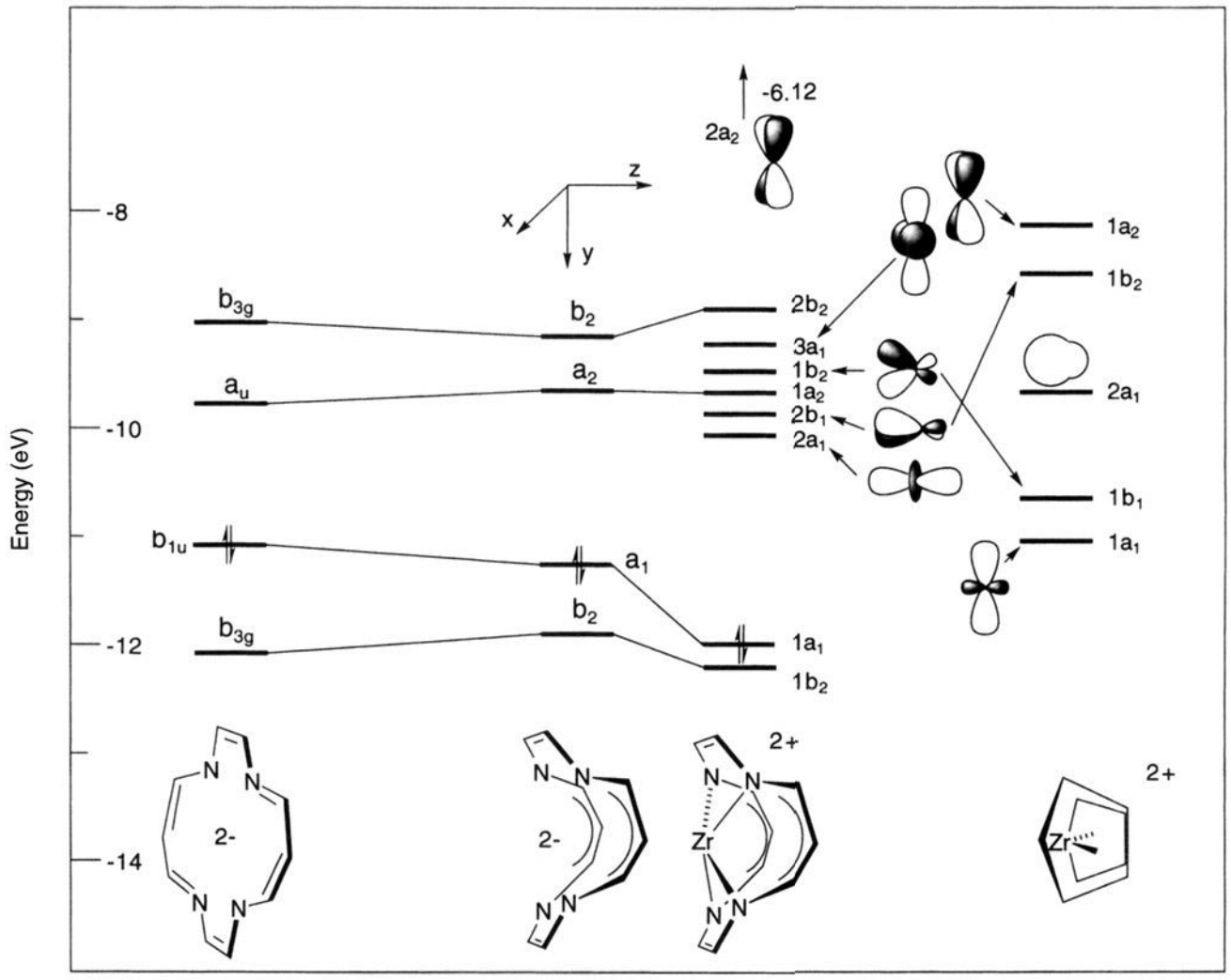

Figure 6. Building of the molecular orbitals of $[Zr(tmtaa)]^{2+}$ step by step.

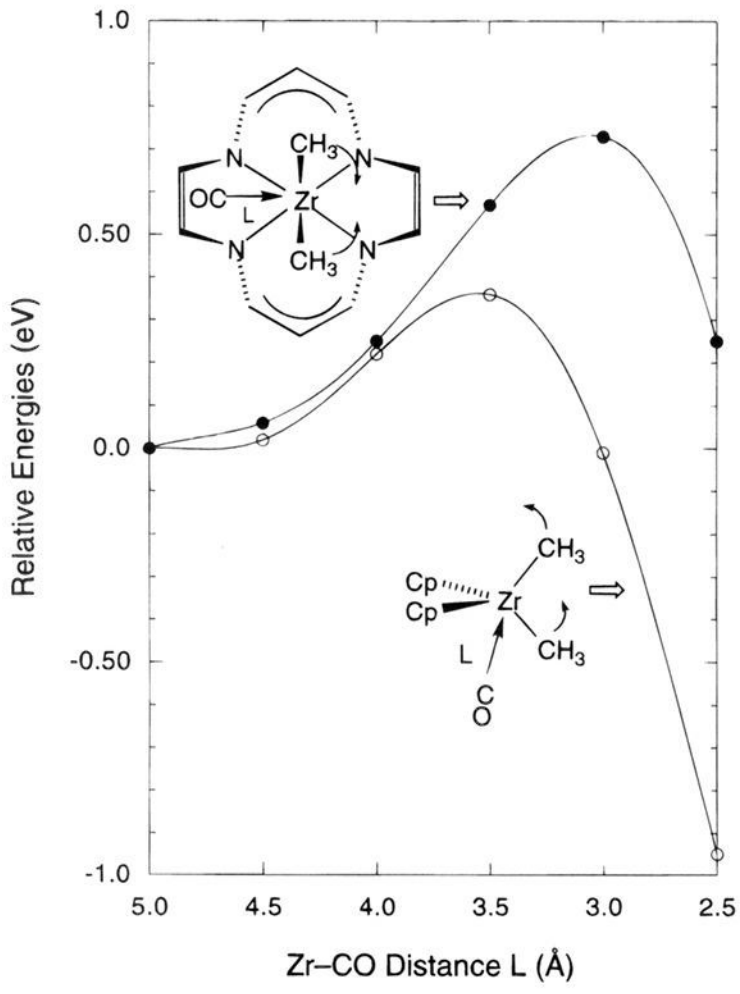

Figure 7. Total energy profile for the favored CO approach toward $[cp_2Zr(CH_3)_2]$[15a] and $[Zr(tmtaa)(CH_3)_2]$.

When considering the electrophilic character of a fragment, atom, or bond, one seeks for the energy change in the molecule when additional charge has been dumped into the LUMO. The higher the contribution of the atom or bond to the LUMO, the more its energy is lowered, and the more electrophilic it is. A partitioning scheme was introduced where the energetic contribution of individual atoms or bonds can be analyzed when

(27) Dronskowski, R.; Hoffmann, R. *Inorg. Chem.* **1992**, *31*, 3107.

Table 9. Net Charges and Electrophilic Indices of $[cp_2Zr]^{2+}$ and $[Zr(tmtaa)]^{2+}$

complex	Zr net charge	Zr ξ^{ele} (meV)
$[cp_2Zr]^{2+}$	+1.52	−10141
$[Zr(tmtaa)]^{2+}$	+0.992	−93921

an electron has been added or removed from the system. The more negative this ξ^{ele} index, the more reactive the atom or bond. The electrophilicity indices computed for $[Cp_2Zr]^{2+}$ and $[Zr(tmtaa)]^{2+}$, as well as the net atomic charge on Zr, are collected in Table 9. Both of these indicators point toward a reduced electrophilicity of $[Zr(tmtaa)]^{2+}$ *vs* $[Cp_2Zr]^{2+}$. The above trends are nicely corroborated by a recent comparative study by Jordan *et al.* $[Cp_2ZrR]^+$ is *ca.* 30 times more active than $[Zr(tmtaa)R]^+$ as an ethylene polymerization catalyst.[7h]

The reaction sequence leading from **3** to **12** and ultimately to **13** illustrates the reactivity of both the zirconium and the iminato carbon in the $[Zr(tmtaa)]^{2+}$ fragment. After coordination of CO to the metal, a migratory insertion occurs, eventually leading to an η^2-acyl. As the metal is not as electrophilic as its $[Cp_2Zr]^{2+}$ analogue, the oxycarbene character ($[Zr]-O-C:-R$) is more pronounced, thus favoring a second insertion, leading to the η^2-ketone **11**. Again here, as the LUMO corresponds to the $1a_2$ orbital, the carbonyl carbon migrates to the iminato carbon. During such a process the $N-C_{iminato}$ overlap population decreases from 0.977 to 0.761 (while for a model amide ZrH_3-NMe_2 we computed a N−C overlap population of 0.771). This bond is cleaved to relieve the ring strain in **12** with concomitant rearrangement, yielding **13**.

Conclusions

Although the saddle shape conformation of the [Zr(tmtaa)] fragment is very reminiscent of the bent $[cp_2Zr]$ moiety, the chemistry we have developed so far emphasizes a number of significant differences: (i) The low-lying d-orbitals on the [Zr(tmtaa)] fragment allow assembling or templating properties very

different in terms of orbitals available and their reciprocal geometrical arrangements. (ii) The electrophilicity in the $[Zr(tmtaa)]^{2+}$ fragment is shared between the metal and the carbons in the imino groups; thus, the metal is a mild, though very efficient, Lewis acid, *i.e.* in the form of $[Zr(tmtaa)(CF_3SO_3)_2]$.[28] In such a form it has been used as a catalyst in aldol condensations and allyl reactions. (iii) The presence of more competitive electrophilic sites on the $[Zr(tmtaa)]^{2+}$ moiety allows the observation of different migration pathways of zirconium-bonded alkyl groups to the tmtaa ligand or to incoming substrates; this is a unique case where the rather complex alkyl migration processes have been elucidated within a macrocyclic-type environment, unlike the case of porphyrin-zirconium derivatives.[8f] (iv) Depending on the nature of the alkyl group and on the reaction solvent, we were able to prevent or to promote the alkyl migration processes, which is fundamental information for those who want to use macrocyclic ligands in organometallic chemistry. (v) The alkyl migration to the ligand ended up with novel forms of tmtaa-derived tri- and tetraanionic macrocyclic N_4 ligands.

Experimental Section

General Procedure. All reactions were carried out under an atmosphere of purified nitrogen. Solvents were dried and distilled before use by standard methods. Infrared spectra were recorded with a Perkin-Elmer 883 spectrophotometer; ^{1}H NMR spectra were measured on a 200-AC Bruker instrument. $[Zr(tmtaa)Cl_2]$ has been prepared according to the published procedure and contains two molecules of THF of crystallization, hereafter not mentioned.

Preparation of 2. MeLi (28 mL of a 0.69 M solution in Et_2O, 19.3 mmol) was added dropwise to a melting suspension of **1** (6.61 g, 10.2 mmol) in benzene (500 mL). The reaction mixture was allowed to reach room temperature while being stirred, was frozen, was thawed again to improve the solid, and then was filtered to remove LiCl. The resulting orange solution was evaporated to dryness, and the orange residue was washed with hexane (100 mL), collected, and dried *in vacuo* (3.20 g, 69.0%). Anal. Calcd for **2**, $C_{24}H_{28}N_4Zr$: C, 62.16; H, 6.09; N, 12.08. Found: C, 62.01; H, 6.20; N, 11.91. ^{1}H NMR (C_6D_6, RT): δ 7.17−6.96 (m, 8H, Ph), 5.05 (s, 2H, CH), 2.00 (s, 12H, CH_3), 0.095 (s, 6H, CH_3 on Zr).

Preparation of 3. $PhCH_2MgCl$ (48 mL of a 0.88 M solution in THF, 42.2 mmol) was added dropwise to a melting suspension of **1** (13.62 g, 21.0 mmol) in benzene (450 mL). Dioxane (20 mL) was added and the reaction mixture was allowed to reach room temperature while being stirred. Volatiles were removed by evaporation *in vacuo*, benzene (650 mL) was added to the resulting orange solid, and the mixture was heated to reflux and filtered while hot; the resulting red solution (from which crystals began to form on cooling to room temperature) was concentrated to 200 mL and kept in the refrigerator overnight, yielding a red microcrystalline product, which was collected, washed with hexane (2 × 50 mL), and dried *in vacuo* (8.48 g, 65.6%). Anal. Calcd for $C_{36}H_{36}N_4Zr$: C, 70.20; H, 5.89; N, 9.10. Found: C, 70.34; H, 5.92; N, 9.26. ^{1}H NMR (C_6D_6, RT): δ 7.26−6.77 (m, 18H, Ph), 4.76 (s, 2H, CH), 1.88 (s, 16H, CH_3, CH_2(benzyl)). ^{1}H NMR (CD_2Cl_2, RT): δ 7.47−6.35 (m, 18H, Ph), 5.03 (s, 2H, CH), 2.24 (s, 12H, CH_3), 1.23 (s, 4H, CH_2(benzyl)). ^{1}H NMR (pyridine-d_5, RT): δ 7.68−6.75 (m, 18H, Ph), 5.05 (s, 2H, CH), 2.21 (s, 12H, CH_3), 1.75 (s, 4H, CH_2(benzyl)).

Preparation of 4 and 6. **2** (2.03 g, 4.38 mmol) was suspended in benzene (70 mL) and refluxed for 3 h (when the mixture reached the boiling point, all the solid dissolved). The resulting red solution was evaporated to dryness *in vacuo*, and the orange residue was washed with hexane (60 mL), collected, and dried *in vacuo* (1.40 g, 69%). Anal. Calcd for **4**, $C_{24}H_{28}N_4Zr$: C, 62.16; H, 6.09; N,12.08. Found: C, 61.88; H, 6.20; N, 11.98. ^{1}H NMR (C_6D_6, RT): δ 7.15−6.68 (m, 8H, Ph), 5.07 (s, 1H, CH), 4.60 (s, 1H, CH), 2.11 (s, 3H, CH_3), 2.07 (s, 3H, CH_3), 1.97 (s, 3H, CH_3), 1.93 (s, 3H, CH_3), −0.25 (s, 3H, CH_3-(methyl on Zr)). Crystals of **6** were obtained as follows: **4** (2.0 g) was dissolved in THF (50 mL), the solvent was removed by evaporation *in vacuo*, and the residue was taken up in toluene (100 mL), giving an orange solution. Crystals of **6** formed on cooling this solution at −30 °C for 4 days. Anal. Calcd for **6**, $C_{28}H_{36}N_4OZr$: C, 62.76; H, 6.77; N, 10.46. Found: C, 62.80; H, 6.81; N, 10.39. ^{1}H NMR (C_6D_6, RT): δ 7.15−6.68 (m, 8H, Ph), 5.08 (s, 1H, CH), 4.59 (s, 1H, CH), 3.54 (m, 4H, THF), 2.13 (s, 3H, CH_3), 2.08 (s, 3H, CH_3), 1.98 (s, 3H, CH_3), 1.93 (s, 3H, CH_3), 1.50 (s, 3H, CH_3), 1.36 (m, 4H, THF), −0.29 (s, 3H, CH_3). ^{1}H NMR (CD_2Cl_2, RT): δ7.27−6.50 (m, 8H, Ph), 5.62 (s, 1H, CH), 4.64 (s, 1H, CH), 3.66 (m, 4H, THF), 2.76 (s, 3H, CH_3), 2.69 (s, 3H, CH_3), 2.21 (s, 3H, CH_3), 1.89 (s, 3H, CH_3), 1.80 (m, 4H, THF), 1.43 (s, 3H, CH_3), −0.92 (s, 3H, CH_3 on Zr).

Preparation of 5. **3** (1.97 g, 3.2 mmol) was suspended in benzene (220 mL), and the mixture was refluxed overnight (when the mixture reached the boiling point, all the solid dissolved). The resulting red solution was evaporated to dryness *in vacuo*, the residue was washed with pentane (170 mL), and the resulting orange powder was collected and dried *in vacuo* (0.901 g, 45.7%). Anal. Calcd for $C_{36}H_{36}N_4Zr$: C, 70.20; H, 5.89; N, 9.10. Found: C, 69.86; H, 6.26; N, 9.17. ^{1}H NMR (C_6D_6, RT): δ 7.33−6.18 (m, 18H, Ph), 4.70 (s, 1H, CH), 4.61 (s, 1H, CH), 3.96 (d, 1H, CH_2(migrated benzyl)), 2.95 (d, 1H, CH_2-(migrated benzyl)), 2.18 (s, 3H, CH_3), 2.03 (s, 3H, CH_3), 1.78 (s, 3H, CH_3), 1.57 (s, 3H, CH_3), 0.95 (m, 2H, CH_2(benzyl on Zr). ^{1}H NMR (pyridine-d_5, RT): δ 7.67−6.41 (m, 18H, Ph), 5.62 (s, 1H, CH), 5.13 (s, 1H, CH), 4.10 (d, 1H, CH_2(migrated benzyl)), 3.48 (d, 1H, CH_2-(migrated benzyl)), 2.65 (s, 3H, CH_3), 2.35 (s, 3H, CH_3), 1.95 (s, 3H, CH_3), 1.62 (d, 1H, CH_2(benzyl on Zr)), 1.57 (s, 3H, CH_3), 1.34 (d, 1H, CH_2(benzyl on Zr)).

Preparation of 7. **3** (2.27 g, 3.69 mmol) was dissolved in THF (200 mL), and the mixture was refluxed for 15 h. Volatiles were removed by evaporation *in vacuo*, and the residue was dissolved in boiling benzene (100 mL), which was filtered while hot; allowing the resulting red solution to stand at room temperature for 4 days afforded a crystalline, pale-orange solid, which was collected and washed with hexane (3 × 50 mL, over 2 h; this operation transformed the solid into a pale-yellow powder, which was dried *in vacuo* (1.51 g, 59.5%)). Anal. Calcd for **7**, $C_{40}H_{44}N_4OZr$: C, 69.83; H, 6.45; N, 8.14. Found: C, 69.83; H, 6.55; N, 8.11. ^{1}H NMR (pyridine-d_5, RT): δ 7.67−6.76 (m, 18H, Ph), 4.86 (s, 2H, CH), 4.43 (d, 2H, CH_2), 3.62 (m, 4H, THF), 3.52 (d, 2H, CH_2), 1.62 (s, 6H, CH_3) overlapping with 1.59 (m, 4H, THF), 1.06 (s, 6H, CH_3). ^{1}H NMR (CD_2Cl_2, RT): δ 7.04−6.52 (m, 18H, Ph), 4.21 (s, 2H, CH), 3.92 (d, 2H, CH_2), 2.85 (d, 2H, CH_2), 2.54 (bm, 4H, THF), 1.97 (s, 6H, CH3), 1.61 (s, 6H, CH_3), 1.23 (bm, 4H, THF). Pyridine-d_5 solutions of **3** and **5** in sealed NMR tubes slowly (2−3 weeks) transform at room temperature into **7** (and some byproducts in 10−25%). Heating samples of **3** in pyridine-d_5 gave complex mixtures only.

Preparation of 8. MeLi (33 mL of a 1.8 M solution in Et_2O, 59.4 mmol) was added dropwise to a melting suspension of **1** (13.10 g, 20.2 mmol) in benzene (500 mL). The reaction mixture was allowed to reach room temperature while being stirred and to stand overnight. LiCl was then removed by careful filtration, THF (10 mL) was added, and the resulting dark brown solution was evaporated to dryness. Hexane (200 mL) was added to the residue, giving (after freezing with liquid N_2) a yellow powder, which was collected and dried *in vacuo* (6.0 g, 47.2%). Anal. Calcd for **8**, $C_{33}H_{47}LiN_4O_2Zr$: C, 62.92; H, 7.52; N, 8.89. Found: C, 62.91; H, 7.52; N, 8.96. ^{1}H NMR (C_6D_6, RT): δ 6.98−6.64 (m, 8H, Ph), 4.73 (s, 2H, CH), 3.04 (m, 8H, THF), 1.89 (s, 6H, CH_3), 1.82 (s, 6H, CH_3), 1.49 (s, 6H, CH_3), 1.09 (m, 8H, THF), 0.187 (s, 3H, CH_3 on Zr). The same product was obtained by adding 1 equiv of LiMe to **4** or **2** in benzene and then recrystallizing the product from hexane/THF. Such a transformation can be followed by ^{1}H NMR in C_6D_6. Crystals suitable for an X-ray analysis were obtained from hexane/THF at −25 °C.

Preparation of 9. **1** (2.06 g, 3.18 mmol) and **3** (2.05 g, 3.33 mmol) were suspended in benzene (130 mL) and stirred overnight at room temperature, giving an orange suspension. The solid was collected, washed with hexane (40 mL), and dried *in vacuo* (2.88 g, 80.8%). Anal. Calcd for **9**, $C_{29}H_{29}ClN_4Zr$: C, 62.17; H, 5.22; N, 10.0. Found: C, 63.22; H, 5.49; N, 9.85. ^{1}H NMR (CD_2Cl_2, RT): equilibrium mixture of **3** (12%), **1** (9%), and **9** (*ca.* 79%), as determined by integration of peaks corresponding to the methyl resonances. The peaks not belonging

(28) Cozzi, P. G.; Floriani, C. *Synlett* **1994**, 857.

to the starting materials are as follows: δ 7.56−6.36 (m, 13H, Ph), 5.41 (s, 2H, CH), 2.38 (s, 12H, CH_3), 1.16 (s, 2H, CH_2(benzyl)).

The same product was obtained following the same procedure as for the preparation of **3** but using only 1 equiv of $PhCH_2MgCl$. This method is less convenient due to the low solubility of the product in benzene, which makes it difficult to separate it from the salts (34%). The product obtained was contaminated with **3**. A sample of **9** was dissolved in pyridine-d_5: the spectrum which was obtained shows the typical pattern of migrated species: δ 7.46−6.75 (m, 13H, Ph), 5.58 (s, 1H, CH), 4.97 (s, 1H, CH), 4.05 (d, 1H, CH_2), 2.84 (d, 1H, CH_2), 2.66 (s, 3H, CH_3), 2.42 (s, 3H, CH_3), 2.29 (s, 3H, CH_3), 1.61 (s, 3H, CH_3). About 5% of **3** could be identified in this solution. In an attempt to eliminate **3**, the product (2.18 g, 3.9 mmol) was dissolved in CH_2Cl_2 (250 mL), benzene (250 mL) was added, and the resulting solution was concentrated to the point a solid started to precipitate (*ca.* 80 mL) and allowed to stand at 8 °C for days. An orange microcystalline powder was then collected and dried *in vacuo* (1 g, 46%). Anal. Calcd for **9**, $C_{29}H_{29}ClN_4Zr$: C, 62.17; H, 5.22; N, 10.0. Found: C, 62.05; H, 5.29; N, 9.77. ^{1}H NMR of a solution obtained dissolving a sample of the recrystallized product in CD_2Cl_2 showed the presence in solution of an equilibrium mixture of **3**, **1**, and **9** in approximately 11%, 14%, and 75%, respectively, thus suggesting the presence of a small amount of **1** in the recrystallized product.

Preparation of 10. **3** (1.37 g, 2.22 mmol) was suspended in toluene (60 mL), and the mixture was cooled to −65 °C. A solution of Bu^{t}NC (0.37 g, 4.46 mmol) in toluene (40 mL) was then added dropwise. The mixture was allowed to warm to room temperature overnight, and the resulting deep red solution was evaporated to dryness *in vacuo* (water bath at room temperature). Hexane (50 mL) was added to the residue, which was collected, washed with more hexane (50 mL), and dried *in vacuo*, giving an ocre powder (1.0 g, 57%). Anal. Calcd for **10**, $C_{46}H_{54}N_6Zr$: C, 70.64; H, 6.96; N, 10.74. Found: C, 70.55; H, 7.29; N, 10.89. ^{1}H NMR (C_6D_6, RT): δ 7.20−6.63 (m, 18H, Ph), 4.92 (s, 2H, CH), 3.91 (d, 2H, CH_2), 2.13 (s, 6H, CH_3), 2.01 (d, 2H, CH_2), 1.92 (s, 6H, CH_3), 0.97 (s, 18H, CH_3-Bu^t). Crystals suitable for the X-ray analysis have been obtained by slow cooling of saturated toluene solutions (from room temperature down to −30 °C). Ligand C=N bands make it impossible to distinguish C=N η^2-iminoacyl bands in their spectrum (from 1590 to lower numbers, large bands in [Zr(tmtaa)(Bz)$_2$]).

Reaction of 3 with CO. Preparation of 12 and 13. **3** (1.76 g, 2.85 mmol) was partially dissolved in THF (70 mL). N_2 was then replaced with CO at room temperature: an immediate reaction took place, with the formation of a red solid. Most of the supernatant was removed, and the wet solid was extracted with boiling CH_2Cl_2 (100 mL). A crystalline solid formed when the resulting solution was allowed to cool slowly and stand for a day. This solid was collected and dried *in vacuo* (0.76 g, 34%). Recrystallization of **12** was carried out in a mixture of CH_2Cl_2/THF = 1/10. Anal. Calcd for **12**, $C_{45}H_{52}N_4O_3Zr$: C, 68.58; H, 6.65; N, 7.11. Found: C, 68.09; H, 6.63; N, 6.95. ^{1}H NMR (CD_2Cl_2, RT): δ 7.21−6.20 (m, 18H, Ph), 5.64 (s, 1H, CH), 5.09 (s, 1H, CH), 3.44 (m, 8H, THF), 3.24 (d, 1H, CH_2), 3.20 (d, 1H, CH_2), 2.92 (d, 1H, CH_2), 2.84 (d, 1H, CH_2), 2.75 (s, 3H, CH_3), 2.66 (s, 3H, CH_3), 2.23 (s, 3H, CH_3), 2.10 (s, 3H, CH_3), 1.72 (m, 8H, THF). A solution of **12** in CH_2Cl_2 slowly evaporated over a period of 2 weeks in a drybox gave **13**·2CH_2Cl_2 as a rather insoluble crystalline solid. The crystals could not be dissolved again in CH_2Cl_2. Anal. Calcd for **13**·2CH_2Cl_2, $C_{76}H_{76}Cl_4N_8O_2Zr_2$: C, 62.62; H, 5.25; N, 7.69. Found: C, 62.31; H, 5.03; N, 7.78. Crystals suitable for an X-ray analysis were obtained from an NMR tube containing a CD_2Cl_2 solution of **12**. Complex **3** absorbs 1 mol of CO *per* zirconium in THF at room temperature, as measured in a gas-volumetric apparatus.

X-ray Crystallography for Complexes 3, 6, 7, and 10. The crystals of compounds **3**, **6**, **7**, and **10** selected for study were mounted in glass capillaries and sealed under nitrogen. The reduced cells were obtained with the use of TRACER.[29] Crystal data and details associated with data collection are given in Tables 1 and S1 (Table S1 is in the supplementary material). Data were collected at room temperature (295 K) for complexes **3**, **6**, and **10** and at T = 143 K for complex **7** on a single-crystal diffractometer (Philips PW1100 for **3** and **6** and Rigaku AFC6S for **7** and **10**, respectively). For intensities and background, individual reflection profiles were analyzed[30] for **7** and **10**, while the "three point technique" was used for **3** and **6**. The structure amplitudes were obtained after the usual Lorentz and polarization corrections,[31] and the absolute scale was established by the Wilson method.[32] The crystal quality was tested by ψ scans showing that crystal absorption effects could be neglected for complexes **3**, **7**, and **10**. The data for complexes **3**, **7**, and **10** were then corrected for absorption using a semiempirical method.[33] The function minimized during the full-matrix least-squares refinement was $\sum w|\Delta F|^2$. A weighting scheme $\{w = k/[\sigma^2(F_o) + g|F_o|^2]\}$ was based on counting statistics[31] for all complexes. Anomalous scattering corrections were included in all structure factor calculations.[34b] Scattering factors for neutral atoms were taken from ref 34a for non-hydrogen atoms and from ref 35 for hydrogen atoms. Among the low-angle reflections, no correction for secondary extinction was deemed necessary.

Solution and refinement were based on the observed reflections. The structures were solved by the heavy-atom method starting from a three-dimensional Patterson map for all complexes. Refinements were first done isotropically and then anisotropically for all non-H atoms, except for the toluene solvent molecule in complex **10**, which was found to be statistically distributed over two positions (A and B) isotropically refined with a site occupation factor of 0.5 applying a rigid body constraint to the rings (A and B) (D_{6h} symmetry). All the hydrogen atoms except for those of toluene in complex **10**, which were ignored, were located from difference Fourier maps and introduced in the final refinement as fixed atom contributions with isotropic U's fixed at 0.10 Å^2 for **3**, **6**, and **10** and at 0.05 Å^2 for **7**. During the refinement the C31−C36 phenyl ring of complex **3** was forced to be a regular hexagon (C−C = 1.395 Å).

The final difference maps showed no unusual feature, with no significant peak having chemical meaning above the general background. Final atomic coordinates are listed in Tables S2−S5 for non-H atoms and in Tables S6−S9 for hydrogens. Thermal parameters are given in Tables S10−S13, and bond distances and angles are given in Tables S14−S17.[36]

Acknowledgment. We would like to thank the "Fonds National Suisse de la Recherche Scientifique" (Grant No. 20-40268.94) for financial support.

Supplementary Material Available: Tables of experimental details associated with data collection and structure refinement (Table S1), final atomic coordinates for non-H and H atoms (Tables S2−S9), thermal parameters (Tables S10−S13), and bond distances and angles (Tables S14−S17) for complexes **3**, **6**, **7**, and **10** and crystal structure (Figure S1) and crystallographic tables (Tables S18−S22) for complex **13** (30 pages); structure factors for complexes **3**, **6**, **7**, **10**, and **13** (40 pages). This material is contained in many libraries on microfiche, immediately follows this article in the microfilm version of the journal, and can be ordered from the ACS; see any current masthead page for ordering information.

JA944198X

(29) Lawton, S. L.; Jacobson, R. A. *TRACER (a cell reduction program)*; Ames Laboratory, Iowa State University of Science and Technology: Ames, IA, 1965.

(30) Lehmann, M. S.; Larsen, F. K. *Acta Crystallogr., Sect. A: Cryst. Phys., Diffr., Theor. Gen. Crystallogr.* **1974**, *A30*, 580−584.

(31) Data reduction, structure solution, and refinement were carried out on an IBM AT personal computer equipped with an INMOS T800 transputer and on an ENCORE 91 computer using: Sheldrick, G.; *SHELX-76. System of Crystallographic Computer Programs*; University of Cambridge: Cambridge, U.K., 1976.

(32) Wilson, A. J. C. *Nature* **1942**, *150*, 151.

(33) North, A. C. T.; Phillips, D. C.; Mathews, F. S. *Acta Crystallogr., Sect. A: Cryst. Phys., Diffr., Theor. Gen. Crystallogr.* **1968**, *A24*, 351.

(34) (a) *International Tables for X-ray Crystallography*; Kynoch Press: Birmingham, England, 1974; Vol. IV, pp 99 and (b) 149.

(35) Stewart, R. F.; Davidson, E. R.; Simpson, W. T. *J. Chem. Phys.* **1965**, *42*, 3175.

(36) See paragraph at the end of this paper regarding supplementary material.